Research Square

Preprints are preliminary reports that have not undergone peer review. They should not be considered conclusive, used to inform clinical practice, or referenced by the media as validated information.

3D food printing of pastes incorporating Jerusalem artichoke puree: formulation, printability, and rheological characterization

Danna M. Vega
Centro de Investigación y Desarrollo en Ciencia y Tecnología de los Alimentos (CIDCA)
Sonia Z. Viña
Centro de Investigación y Desarrollo en Ciencia y Tecnología de los Alimentos (CIDCA)
Maria Alejandra Garcia
magarcia@quimica.unlp.edu.ar

Centro de Investigación y Desarrollo en Ciencia y Tecnología de los Alimentos (CIDCA)

Research Article

Keywords: food additive manufacturing, Jerusalem artichoke, extrudable food pastes, rheological properties, texture profile analysis, functional ingredients, gluten-free foods

Posted Date: July 6th, 2026

DOI: https://doi.org/10.21203/rs.3.rs-10009367/v1

License: This work is licensed under a Creative Commons Attribution 4.0 International License.
Read Full License

Additional Declarations: No competing interests reported.

3D food printing of pastes incorporating Jerusalem artichoke puree: formulation, printability, and rheological characterization

Danna Mikaela Vega [(1)(2)], Sonia Zulma Viña [(1)(3)], María Alejandra García [(1) *]

[(1)] Centro de Investigación y Desarrollo en Ciencia y Tecnología de los Alimentos (CIDCA), Facultad de Ciencias Exactas UNLP, CONICET, CIC-PBA, 47 y 116, La Plata (1900), Buenos Aires, Argentina.

[(2)] Departamento de Ingeniería Química, Facultad de Ingeniería UNLP, 1 y 47, La Plata (1900), Buenos Aires, Argentina.

[(3)] Curso Bioquímica y Fitoquímica, Facultad de Ciencias Agrarias y Forestales UNLP, 60 y 119, La Plata (1900), Buenos Aires, Argentina.

[*] Corresponding author: magarcia@quimica.unlp.edu.ar

ORCID: D.M. Vega: 0009-0001-7264-8338

S.Z. Viña: 0000-0002-2948-5609

M.A. García: 0000-0002-4292-7889

Abstract

Jerusalem artichoke (*Helianthus tuberosus* L.) is a carbohydrate-rich tuber with high inulin content, offering potential for structuring functional food matrices. This study evaluated its incorporation into extrusion-based 3D food printing systems through partial replacement (20-40% w/w) of dehydrated potato. Rheological analysis showed a decrease in elastic modulus from 15.74 ± 1.05 kPa (control) to 6.31 ± 0.53 kPa at 40% substitution, indicating reduced rigidity. However, xanthan-pectin addition restored viscoelastic balance and enabled stable extrusion and shape retention. Linear viscoelastic and thixotropic responses were associated with printability and structural recovery. Post-printing ionotropic gelation with calcium chloride significantly increased hardness (from 0.28±0.03 N to 1.41±0.44 N) and improved structural integrity. Formulations containing up to 40% Jerusalem artichoke puree maintained multilayer buildability and geometric fidelity comparable to the control. These results demonstrate that Jerusalem artichoke puree can be used to design gluten-free, prebiotic-rich printable foods with tunable mechanical properties.

Keywords: food additive manufacturing; Jerusalem artichoke; extrudable food pastes; rheological properties; texture profile analysis; functional ingredients; gluten-free foods

1. Introduction

Three-dimensional (3D) food printing has emerged as a disruptive manufacturing technology capable of producing foods with controlled geometry, spatial architecture, and tailored composition, enabling new approaches to personalization and functional design in food systems (Sun et al., 2015; Zhu et al., 2023). Unlike conventional food processing, the success of 3D food printing is strongly governed by the physicochemical and rheological properties of the printing material, commonly referred to as extrudable food pastes.

These pastes act as edible feedstocks whose flow behavior, viscoelastic balance, and structural recovery determine printability, shape fidelity, and post-deposition stability of the printed constructs (Jeon et al., 2024). In particular, adequate yield stress, shear-thinning behavior, and elastic recovery, typically associated with storage modulus values in the order of kPa and rapid structural recovery after shear, are critical requirements to ensure continuous deposition while preventing structural collapse (Liu et al., 2017). Accordingly, formulation strategies are a key determinant of process robustness and reproducibility in 3D food printing.

To date, most studies on extrudable food pastes have focused on starch-rich matrices, with mashed potato and potato-based systems being among the most extensively investigated due to their favorable rheological properties and widespread availability (Cui et al., 2022). However, the exploration of alternative carbohydrate sources capable of partially replacing conventional potato-based matrices remains limited, despite the need to diversify raw materials, improve nutritional functionality, and reduce reliance on starch-rich systems with limited health benefits. Moreover, achieving printability with such alternative matrices typically requires the rational incorporation of hydrocolloids to tailor viscosity, yield behavior, and structural recovery; among them, xanthan gum is widely used in extrusion-based edible inks due to its pronounced shear-thinning behavior and its ability to promote shape fidelity after deposition (Abu Elella et al., 2021; Cai et al., 2023; Hakim et al., 2024).

In addition to rheological structuring, post-printing stabilization strategies play a key role in maintaining the integrity of complex printed geometries. One effective approach is chemical gelation, which enables the transformation of a malleable, extruded material into a stable three-dimensional network. In this context, low-methoxyl pectin is particularly relevant due to its ability to undergo ionic crosslinking with divalent cations such as calcium, a mechanism that has been widely applied in hydrocolloid-based systems to improve mechanical stability, often resulting in increased gel strength and resistance to deformation after deposition (Prithviraj et al., 2025). Beyond its technological function, calcium-mediated gelation may also contribute to the nutritional profile of the final product by increasing calcium availability.

In this context, Jerusalem artichoke (*Helianthus tuberosus* L.) represents a carbohydrate-rich tuber with high inulin content, offering opportunities to modulate texture and functional performance in structured food matrices. Inulin is a well-established prebiotic compound associated with beneficial effects on gut health, and its incorporation into printable food matrices enables the development of functional structures without compromising processability, which remains a key challenge in extrusion-based 3D food printing (Kaur & Gupta, 2002). Despite these advantages, its potential application as a matrix component in extrudable pastes for 3D food printing has not yet been systematically investigated.

Therefore, the objective of this study was to develop and characterize extrudable pastes suitable for 3D food printing by partially replacing dehydrated potato with Jerusalem artichoke puree. The effects of formulation on rheological behavior, structural recovery after extrusion, printability, and textural properties of the printed products were evaluated, aiming to assess the feasibility of producing gluten-free, prebiotic-enriched foods with complex geometries.

2. Materials and Methods

2.1 Materials

Fresh Jerusalem artichoke (JA) tubers, from the white variety, were harvested in La Plata, Buenos Aires, Argentina (Experimental Station Julio Hirschhorn, Facultad de Ciencias Agrarias y Forestales UNLP, 34°58′ S, 57°54′ W). Commercial dehydrated potato flakes (El Peoncito, Alimentos Villares S.A.C., Argentina) were used as the reference starch-based matrix. Xanthan gum (Onza de Oro, Condiment S.A., Argentina) and low-methoxyl pectin (commercial grade, Gelfix S.A., Argentina) were used as hydrocolloids. Calcium chloride ($CaCl_2$) (analytical grade, Anedra S.A., Buenos Aires, Argentina) was used to induce chemical gelation.

2.2 Preparation of Jerusalem Artichoke Powder

JA tubers were washed under running tap water to remove soil residues and sanitized by immersion in a sodium hypochlorite solution (NaClO, 385 ppm) for 10 min. Superficial incisions were made on the peel, and tubers were cooked in an electric pressure cooker (OPAT22P, ATMA, Argentina) for 20 min, using a tuber-to-water ratio of 1:2 (w/w). After cooking, tubers were rapidly cooled in cold water (≈4°C) to facilitate skin removal. The peel was manually removed, and the pulp was mashed using a household potato masher (Liliana, Argentina) to obtain a homogeneous puree. The puree was dehydrated for 19 h using a food dehydrator (MAQUINARIAS COBO, Argentina) under a three-step drying program consisting of successive stages at 66 °C (2 h), 56 °C (2 h), and 43 °C (15 h), then milled (HC-250Y DAMAI grinder, China), sieved (35-mesh sieve), and re-milled to obtain a fine powder. The dried JA powder was stored in airtight containers at 20°C until use.

2.3 Chemical Composition of Jerusalem Artichoke Powder

Moisture, ash, total protein, and lipid contents of JA powder were determined in triplicate according to AOAC standard methods (1990), as described previously by Vega et al. (2024).

2.4 Formulation of Extrudable Pastes

Extrudable pastes were formulated using commercial dehydrated potato (DP) flakes, JA powder, and their blends. DP was partially replaced by JA powder at levels of 20% and 40% (w/w). All formulations were reconstituted to a total solid concentration of 20% (w/w).

Hydrocolloids were incorporated as follows: xanthan gum (1.0% w/w, based on total solids) and/or low-methoxyl pectin (1.2% w/v in the reconstitution liquid). Preliminary rheological screening of potato-based pastes was performed by varying xanthan gum concentration (0, 0.5, 1.0, and 2.0% w/w, based on total solids) and evaluating the evolution of the storage (G′) and loss (G″) moduli as a function of oscillatory strain and angular frequency. Based on this screening, the combined xanthan gum-pectin formulation was selected as the structural basis for all pastes containing JA powder, including partial replacements of DP and the 100% JA powder formulation.

In the preparation of the extrudable pastes, reconstitution liquids (hydrocolloid solutions) were heated to approximately 70 °C prior to mixing. Solid ingredients were hydrated and manually mixed for 5 min, then allowed to rest for 1 min to ensure full hydration. A total mass of 150 g was prepared for each formulation. The compositions of the different paste formulations are summarized in **Table 1**.

Table 1. Composition of extrudable paste formulations used for 3D food printing

Formulation code	DP (g)	JAP (g)	XG (g)	Reconstitution liquid (125 mL, ~70 °C)
MP	25	0	0	Water
MP-XG	25	0	1.5	Water
MP-LMP	25	0	0	LMP solution (1.2% w/v)
MP-XG-LMP	25	0	1.5	LMP solution (1.2% w/v)
MP80-JAP20	20	5	0	Water
MP80-JAP20-LMP	20	5	0	LMP solution (1.2% w/v)

MP80-JAP20-XG-LMP	20	5	1.5	LMP solution (1.2% w/v)
MP60-JAP40-XG-LMP	15	10	1.5	LMP solution (1.2% w/v)
JAP-XG-LMP	0	25	1.5	LMP solution (1.2% w/v)

Note: All quantities correspond to a total batch mass of approximately 150 g of extrudable paste (total solids ≈ 20% w/w). MP: mashed potato; DP: dehydrated potato flakes; JAP: Jerusalem artichoke powder; XG: xanthan gum; LMP: low-methoxyl pectin

2.5 Rheological Characterization of Extrudable Pastes

Rheological measurements were performed using a controlled-stress rheometer (TA Instruments HR-20, USA) equipped with smooth parallel plate geometry (gap: 1 mm). All tests were conducted at 25 °C and measurements were performed in duplicate, from two independent sample preparations.

Rotational flow tests were performed to obtain steady-state flow curves for the formulated pastes. Samples were equilibrated at the test temperature for 3 min prior to measurement, and shear rate was varied from 0.0001 to 1 s^{-1} over a total duration of 3 min.

Regarding the oscillatory mode tests, strain amplitude sweep tests were initially performed to determine the linear viscoelasticity range (LVR). For this, the sample was first held at 25°C for 60 seconds, and then the LVR was determined at a frequency of 1 Hz recording the storage (G') and loss (G'') moduli. Through these tests, the effect of the structural components of the pastes was also studied, analyzing the evolution of the modules (G′ and G″) as a function of the oscillatory deformation for the control potato-based paste (MP, mashed potato), the potato paste with xanthan gum (MP-XG), the potato paste reconstituted with low methoxyl pectin solution (MP-LMP) and the formulation containing both hydrocolloids (MP-XG-LMP).

In addition, strain sweep tests were used to determine the flow point of each material, defined as the strain at the G′-G″ crossover (G′ = G″).

Next, a strain value corresponding to the LVR was selected, and frequency sweeps were performed in a range from 0.01 to 100 Hz, recording G' and G'' moduli. In this case, the sample was also stabilized for 60 seconds at the measurement temperature prior to the start of the test.

Elastic recovery and structural stability of the extrudable pastes under conditions representative of the printing process were evaluated by a three-interval time sweep test (3ITT) in oscillatory mode. The test consisted of three consecutive 60-s intervals performed at a constant frequency of 1 Hz. The first and third intervals were conducted within the LVR at a strain of 0.2%, corresponding to pre- and post-printing resting conditions. The intermediate interval was performed outside the LVR at a strain of 10%, simulating the high deformation experienced during extrusion. This protocol allowed the assessment of structural breakdown and subsequent recovery of the pastes, which is directly related to shape fidelity of the printed constructs. Storage and loss moduli were continuously recorded. The structural recovery ratio was calculated as the quotient between the average values of the elastic modulus (G') in step 3 and those corresponding to step 1 of the 3ITT test.

2.6 3D Food Printing and Post-Printing Gelation

Printing was carried out using a food-grade 3D printer (CHIMAK 3D, Argentina) operated at a printing speed of 5 rpm, with a nozzle diameter of 2 mm and a layer height of 1-2 mm, parameters that were selected from preliminary experiments. To optimize post-printing chemical gelation, cylindrical discs (approximately 3 mm height, three printed layers, and 2.5 cm diameter) were printed. Chemical gelation was induced by spraying calcium chloride solutions at concentrations of 1, 5, and 10% (w/v) onto the printed structures.

2.7 Texture Profile Analysis of Printed Products

Texture profile analysis (TPA) was performed on the 3D-printed and calcium-gelled samples obtained as described in Section 2.6, using a Brookfield CT3 Texture Analyzer (Middleboro, MA, USA) equipped with a SMSP/25 probe (25.4 mm in diameter; 38.1 mm in height). Hardness, cohesiveness, elasticity, and adhesiveness were determined following the procedure described by Vega et al. (2024). At least eight replicates were analyzed for each formulation.

2.8 Printing of Complex Geometries

The printability of complex digital geometries was evaluated using three-dimensional models obtained from a digital library (Thingiverse) in STL format. The models were converted into printer-specific G-code files using the open-source slicing software Slic3r (version 1.3.0). Shape fidelity of the printed structures was quantitatively evaluated after calcium-induced gelation. Dimensional deviation (%) was calculated as the relative difference between the measured and designed dimensions On the printed samples dimensions were measured directly using a digital caliper, and results were expressed as mean ± standard deviation from at least six independent samples.

2.9 Statistical Analysis

Data obtained from chemical composition, rheological, and textural measurements were analyzed using one-way analysis of variance (ANOVA). When significant differences were detected, means were compared using Fisher's least significant difference (LSD) test at a significance level of $\alpha = 0.05$. Statistical analyses were performed using InfoStat software (Di Rienzo et al., 2011)

3. Results and Discussion

3.1 Chemical composition of Jerusalem artichoke powder

The proximate composition of JA powder revealed a moisture content of 4.51 ± 0.03% and a predominant carbohydrate fraction (78.26 ± 0.33%, calculated by difference), with protein, ash, and lipid contents of 10.52 ± 0.04%, 5.39 ± 0.17%, and 1.32 ± 0.12% (wet basis), respectively. This carbohydrate-centric profile is intrinsically linked to the biochemical nature of *H. tuberosus tubers*, which are characterized by the accumulation of high levels of inulin-type fructans (linear β (2→1)-linked D-fructose polymers) that may constitute up to approximately 80% of the total dry matter (Rubel et al., 2018; Shariati et al., 2021). Such inulin-rich fractions are key determinants of the technological functionality of JA powders, influencing properties such as viscosity, solubility, and structural stability during food processing (Afoakwah, 2022; Rubel et al., 2018). In this context, the present results contribute to the still limited body of literature addressing the proximate characterization of JA powder as a raw material, complementing previous reports on tuber-derived powders. Moreover, the observed composition is consistent with recent applications of JA flour aimed at enhancing fiber and functional carbohydrate content in complex food systems, including gluten-free baked products (Vega et al., 2024)

3.2 Rheological Characterization of Extrudable Pastes

Rheological properties of the extrudable pastes are critical for successful 3D food printing, as the material must exhibit appropriate viscosity to ensure extrusion through the printing nozzle, while simultaneously presenting adequate structural strength to promote interlayer adhesion and maintain shape fidelity after deposition (Hu et al., 2023; Liu, Zhang, et al., 2018). In this context, parameters such as the linear viscoelastic region (LVR), flow point, viscoelastic moduli, and frequency dependence provide key insights into printability and structural reliability of the printed constructs (Letras et al., 2022).

Strain (amplitude) sweep tests were used to determine the LVR and the flow point of the different formulations, defined as the strain at the G′-G″ crossover (G′=G″). The crossover of G″ above G′ indicates disruption of the network structure and the onset of flow (Mezger, 2020).

When evaluating the effect of xanthan gum concentration, a non-monotonic influence on the viscoelastic stability of potato-based pastes was observed. Increasing the xanthan gum content to 1.0% (w/w) resulted in a significant increase ($p<0.05$) in both the strain at which the crossover point is observed and the G′-G″ values at that point, indicating greater resistance to deformation and a more cohesive network structure (**Figure 1a**). In contrast, further increasing xanthan gum concentration to 1.5-2.0% did not provide additional reinforcement, as evidenced by a reduction in crossover strain and no significant ($p>0.05$) increase in crossover modulus compared to the control (**Table insert in Figure 1a**). These results suggest the existence of an optimal xanthan gum concentration around 1.0%, beyond which excessive structuring may promote brittleness rather than improved deformation tolerance.

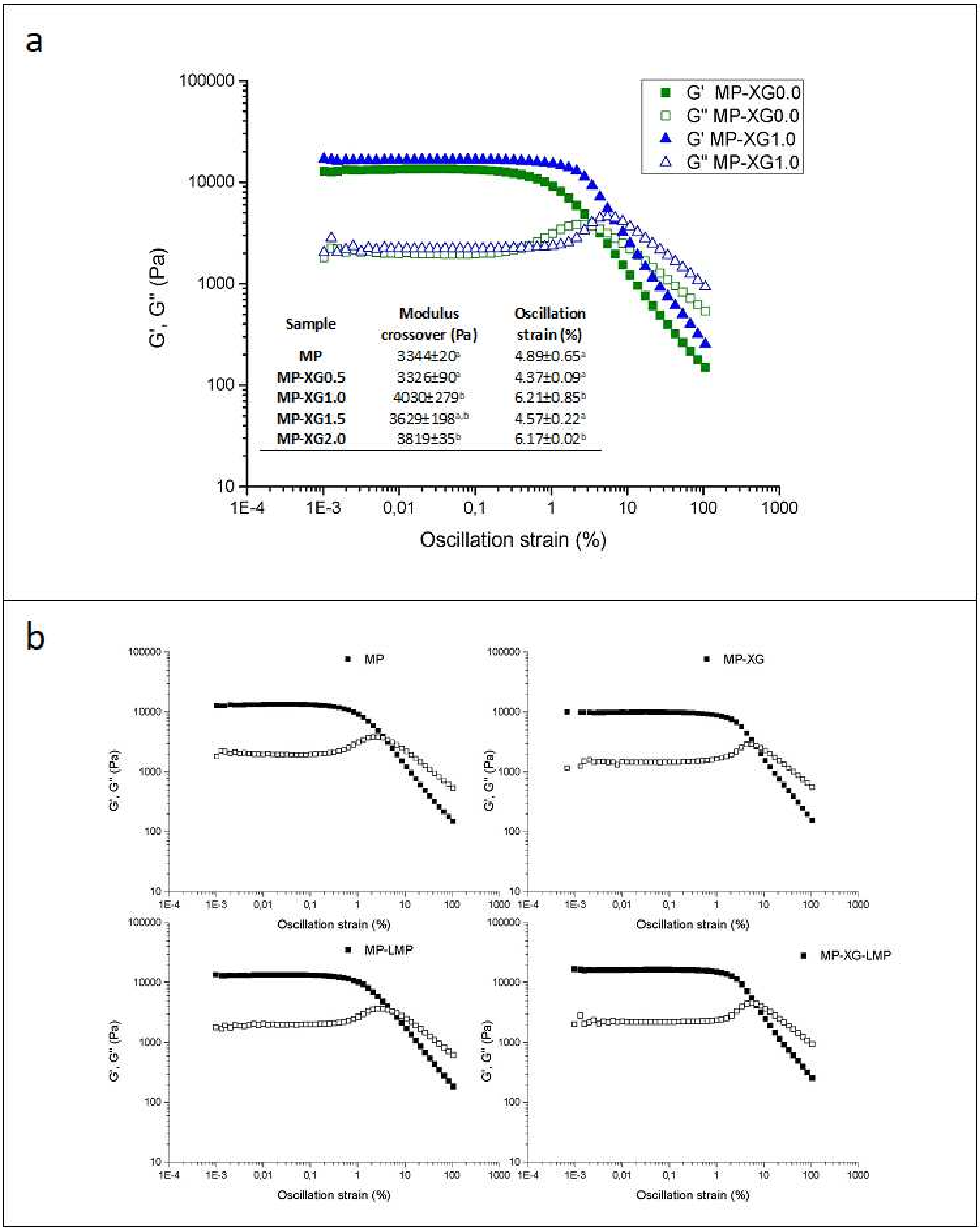

Figure 1. The Y-axis, G' (filled symbol) and G'' (empty symbol), correspond to the storage and loss modules respectively. MP: mashed potatoes; XG: xanthan gum. **a:** Strain amplitude sweep for extrudable pastes. XG-xx: xanthan gum at xx% w/w. **b:** Strain amplitude sweep for extrudable pastes. XG: xanthan gum at 1% w/w; LMP: low methoxyl pectin at 1% w/w.

A comparative analysis among the different hydrocolloid systems revealed clear differences between MP, MP-XG, MP-LMP, and MP-XG-LMP formulations in terms of both the strain at the G′-G″ crossover and the modulus value at this transition point (**Figure 1b**). The control formulation (MP) exhibited a crossover at 3.96 ± 0.23% strain, indicating early structural breakdown under oscillatory deformation (**Table insert in Figure 1b**). The incorporation of xanthan gum (MP-XG) significantly shifted the crossover toward higher strain values (6.28 ± 0.36%), reflecting enhanced resistance to deformation, although this transition occurred at a lower crossover modulus compared to the control. In contrast, the addition of pectin alone (MP-LMP) produced a more moderate effect, with crossover strain values (4.89 ± 0.65%) statistically similar to those of MP, suggesting limited reinforcement of deformation tolerance. Notably, the combined use of xanthan gum and pectin (MP-XG-LMP) resulted in the highest crossover modulus (4556 ± 86 Pa) together with an increased crossover strain (5.77 ± 1.16%), suggesting a synergic effect of both hydrocolloids and the formation of a more cohesive and mechanically robust viscoelastic network. These results highlight the distinct and complementary roles of the used hydrocolloids, with xanthan gum primarily enhancing deformation tolerance and the combined hydrocolloid system promoting a stronger and more resistant structure. LMP, for its part, is the hydrocolloid that provides the ability to gel in Ca ion presence. Xanthan gum solutions have been described as adopting a rod-like conformation in water and, at sufficiently high concentrations, may exhibit an apparent yield stress in addition to pronounced shear-thinning behavior (Whitcomb & Macosko, 1978; Cai et al., 2023), which is advantageous for extrusion-based deposition. While xanthan gum is primarily used as a thickener and rheology modifier rather than a standalone gelling agent, LMP can form ionically crosslinked gel networks in the presence of Ca^{2+}, providing a post-deposition stabilization route for printed structures. Based on these findings, the combined hydrocolloid system (XG and LMP) was selected for subsequent formulations incorporating JA powder, including partial replacements and the 100% JA paste, in order to ensure sufficient structural stability and deformation tolerance during extrusion-based printing.

Based on the viscosity curves obtained from rotational rheological tests (**Figure S1**), the pastes exhibited shear-thinning (pseudoplastic) behavior with an apparent yield stress. Such rheological behavior is widely recognized as a key requirement for extrusion-based 3D printing processes, as it facilitates extrusion under shear while supporting shape retention after deposition (Qin et al., 2025).

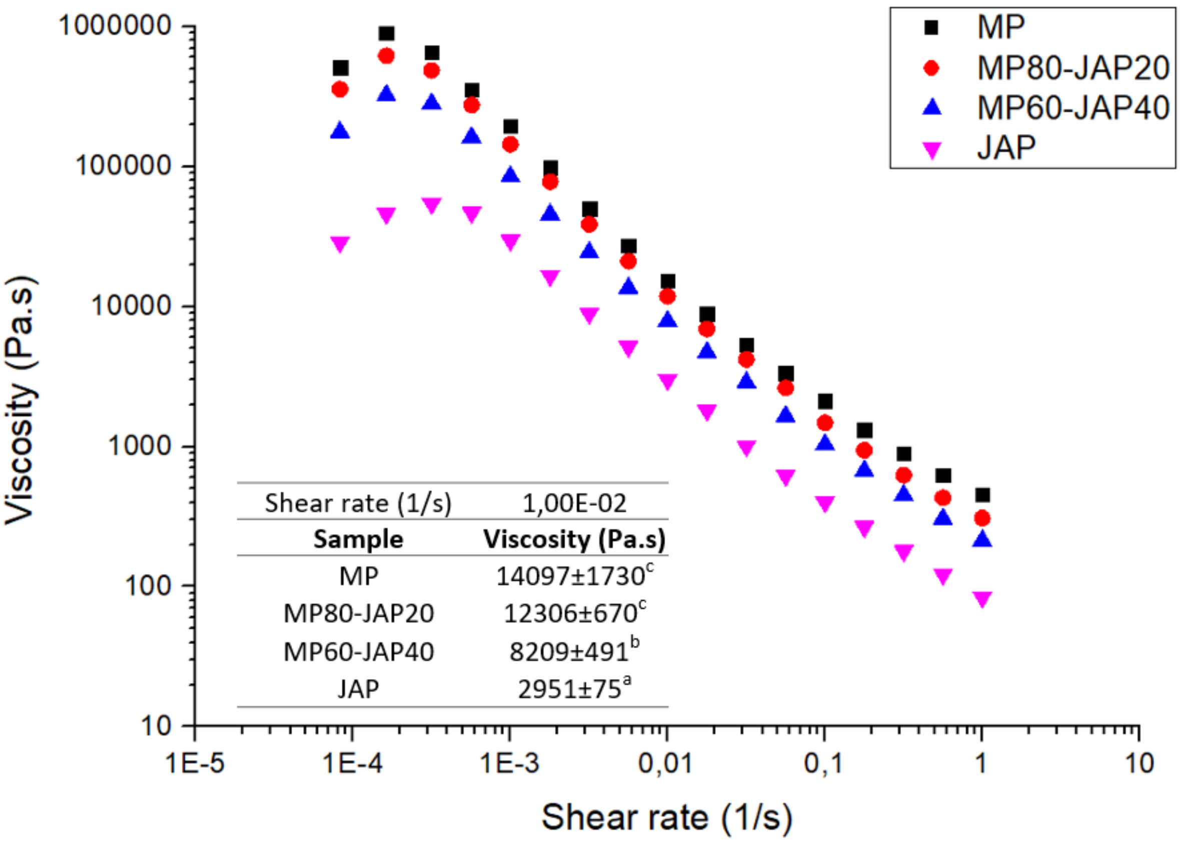

Shear rate (1/s)	1,00E-02
Sample	**Viscosity (Pa.s)**
MP	14097±1730[c]
MP80-JAP20	12306±670[c]
MP60-JAP40	8209±491[b]
JAP	2951±75[a]

Figure S1. Flow curves of extrudable pastes. MP: mashed potatoes; JAP: Jerusalem artichoke puree; MP80-JAP 20: 20% replacement with JAP; MP60-JAP 40: 40% replacement with JAP.

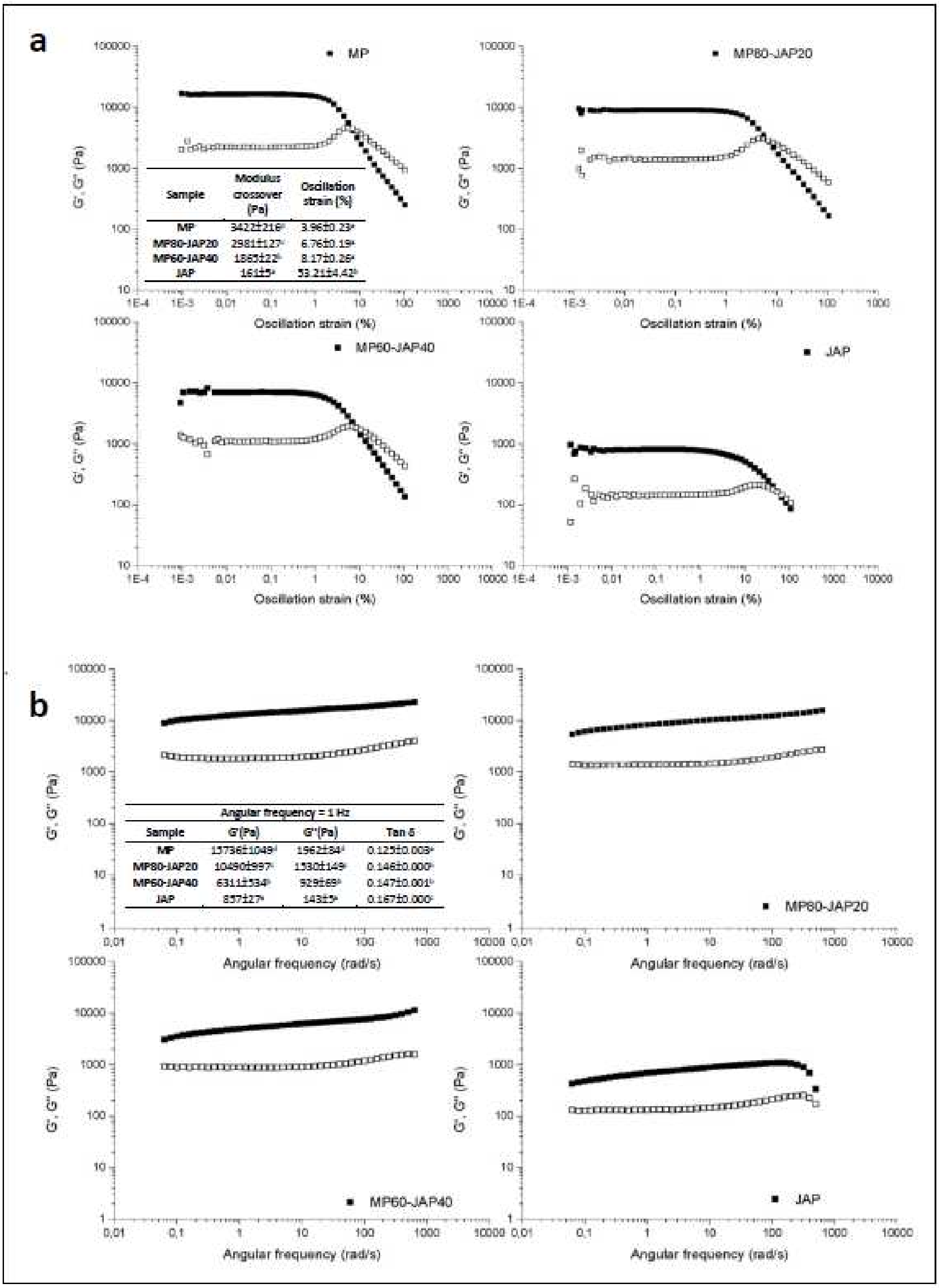

Sample	Modulus crossover (Pa)	Oscillation strain (%)
MP	3422±216[d]	3.96±0.23[a]
MP80-JAP20	2981±127[c]	6.76±0.19[a]
MP60-JAP40	1865±22[b]	8.17±0.26[a]
JAP	161±5[a]	53.21±4.42[b]

Angular frequency = 1 Hz			
Sample	G'(Pa)	G''(Pa)	Tan δ
MP	15736±1049[d]	1962±84[d]	0.125±0.003[a]
MP80-JAP20	10490±997[c]	1530±149[c]	0.146±0.000[b]
MP60-JAP40	6311±534[b]	929±69[b]	0.147±0.001[b]
JAP	857±27[a]	143±5[a]	0.167±0.000[c]

Figure 2. The Y-axis, G' (filled symbol) and G'' (empty symbol), correspond to the storage and loss modules respectively. MP: mashed potatoes; JAP: Jerusalem artichoke puree; MP80-JAP20 and MP60-JAP40 represent formulations with a 20% and 40% replacement of MP by JAP. **a:** Strain amplitude sweep for extrudable pastes. **b:** Frequency sweeps for extrudable pastes.

As shown in **Figure 2a**, for the MP-based paste, the flow point occurred at *approximately* 6% strain, whereas for the JA paste this value shifted to around 53% strain. This pronounced displacement suggests that MP exhibits a more fragile structure, while the incorporation of JA (>20%) increases resistance to deformation, which could favor extrusion-based printing by delaying structural breakdown (**Figure 2a**).

Although JA paste exhibited a broader LVR, the absolute values of G′ and G″ were lower than those of the other formulations (**Table insert in Figure 2a**). This indicates that, while JA paste forms a network capable of tolerating larger deformations, it is structurally weaker and less rigid, which is consistent with the steady-state flow curves (**Figure S1**). These rheological features can be interpreted in light of the chemical composition of JA paste. As discussed previously, JA powder is characterized by a high total carbohydrate content, largely associated with inulin-type fructans. Unlike starch-rich potato-based matrices, these soluble and fiber-like carbohydrates contribute less to the formation of a rigid, load-bearing network, which may explain the lower absolute values of G′ and G″ observed for JA-based formulations, despite their greater tolerance to deformation. Similar effects of inulin-rich fractions on weakening elastic networks while promoting deformability have been reported in other food systems, highlighting their role in modulating viscoelastic balance rather than providing structural rigidity (Juszczak et al., 2012; Paseephol et al., 2008).

Mechanical spectra obtained from frequency sweep tests (**Figure 2b**) showed that MP, MP80-JAP20, and MP60-JAP40 formulations displayed the typical behavior of weak gels, characterized by G′ values higher than G″ across the frequency range and a separation of approximately one logarithmic cycle between both moduli. This viscoelastic response has been widely reported for printable food matrices (Letras et al., 2022; Liu, Zhang, et al., 2018; Uribe-Wandurraga et al., 2021). Increasing the proportion of JA puree resulted in a marked decrease in both G′ and G″, while maintaining a similar frequency dependence up to 40% JA powder. In contrast, the formulation containing 100% JA powder exhibited a significantly weaker structural network and a higher frequency dependence, showing structural breakdown at frequencies close to 200 rad/s. The weaker viscoelastic structure observed in JA-containing formulations may be attributed to differences in polymer-polymer and polymer-water interactions within the matrix. In potato-based systems, gelatinized starch provides a continuous phase capable of forming entangled and hydrogen-bonded networks that interact synergistically with hydrocolloids, resulting in higher G′ values and greater mechanical strength (Megusar et al., 2022). In contrast, the carbohydrate fraction of JA is dominated by inulin-type fructans and shorter fructooligosaccharides, which are highly soluble and exhibit limited chain entanglement. These low-molecular-weight carbohydrates compete for water but contribute less to network formation, thereby reducing the effectiveness of hydrocolloid structuring and leading to a weaker viscoelastic matrix (Karimi et al., 2015; Witczak et al., 2014).

The values of G′ and G″ measured at 1 Hz (**Table insert in Figure 2b**) confirmed a significant decrease ($p<0.05$) in both moduli as the proportion of JA powder increased. This reduction in mechanical strength could facilitate extrusion by lowering the energetic demand on the printing system; however, it must be carefully balanced to avoid compromising shape fidelity of the printed structures.

The dynamic loss tangent ($\tan \delta = G''/G'$) ranged between 0.14 and 0.19 for all formulations, in agreement with values previously reported for printable food pastes (Liu, Bhandari, et al., 2018). Tan δ values lower than 1 indicate a predominantly elastic behavior, which is desirable for maintaining structural integrity after printing (Hu et al., 2023). A significant increase in tan δ ($p<0.05$) was observed with increasing JA powder content, indicating a higher viscous contribution. This effect is consistent with the compositional characteristics of JA powder and may be associated with the presence of soluble dietary fiber, particularly inulin, which can modify intermolecular interactions within the matrix and increase the relative viscous contribution of the system, as previously discussed.

3.3 Three-interval thixotropy test

The thixotropic behavior and structural recovery capacity of extrudable pastes intended for extrusion-based 3D food printing can be effectively evaluated using a three-interval thixotropy test (3ITT). This oscillatory protocol provides insight into the ability of the material to rebuild its internal structure after being subjected to a high shear deformation exceeding the yield-like region, which is critical for shape fidelity after printing. Moreover, the test allows simulation of three relevant states of the paste: pre-printing rest, extrusion through the nozzle, and post-deposition recovery (del-Mazo-Barbara & Ginebra, 2021).

Figure 3 shows the results of the three-interval tests performed on the developed extrudable pastes. All formulations exhibited the expected viscoelastic pattern, with $G' > G''$ during the resting intervals (intervals 1 and 3) and $G'' > G'$ during the intermediate high-strain interval. This behavior is considered desirable for extrusion-based printing, as it reflects a solid-like response during rest, which is necessary for paste stability prior to printing and for the self-supporting capacity of the printed structures, and a liquid-like response under high deformation, which facilitates extrusion through the printing nozzle.

All formulations showed the ability to recover their structure after shear cessation, indicating a certain degree of structural resilience and suggesting adequate shape reliability of the printed constructs. Structural recovery ratios of extrudable pastes were 0.93±0.14 and 0.97±0.01 for MP and JA based pastes, respectively. Nevertheless, notable differences were observed depending on the incorporation level of JA powder. Blended formulations containing 20% and 40% JA powder exhibited a slight delay in structural recovery compared to the control formulation (**Figure 3b**), which is characteristic of thixotropic systems where network rebuilding is not instantaneous (Bohórquez Montoya, 2018). In this case, the structural recovery ratios were 0.93±0.02 and 0.99±0.07 for 20JA and 40JA based pastes, respectively. This delayed recovery is consistent with the rheological trends discussed previously and may be associated with the compositional features of JA powder. As reported in the compositional analysis, this ingredient is rich in soluble dietary fiber, particularly inulin, which exhibits a high water-holding capacity (Vega et al., 2024). The presence of these fiber fractions may alter water availability and interfere with hydrocolloid-starch interactions, thereby hindering the formation of a more cohesive three-dimensional network. This effect is reflected in the lower G′ values observed for JA powder-rich formulations and in their slower post-shear recovery (**Figure 3b**). In contrast, the control paste (MP-based formulation) displayed a more cohesive structure and faster recovery, indicating a stronger and more interconnected network promoted by the combination of starch and hydrocolloids.

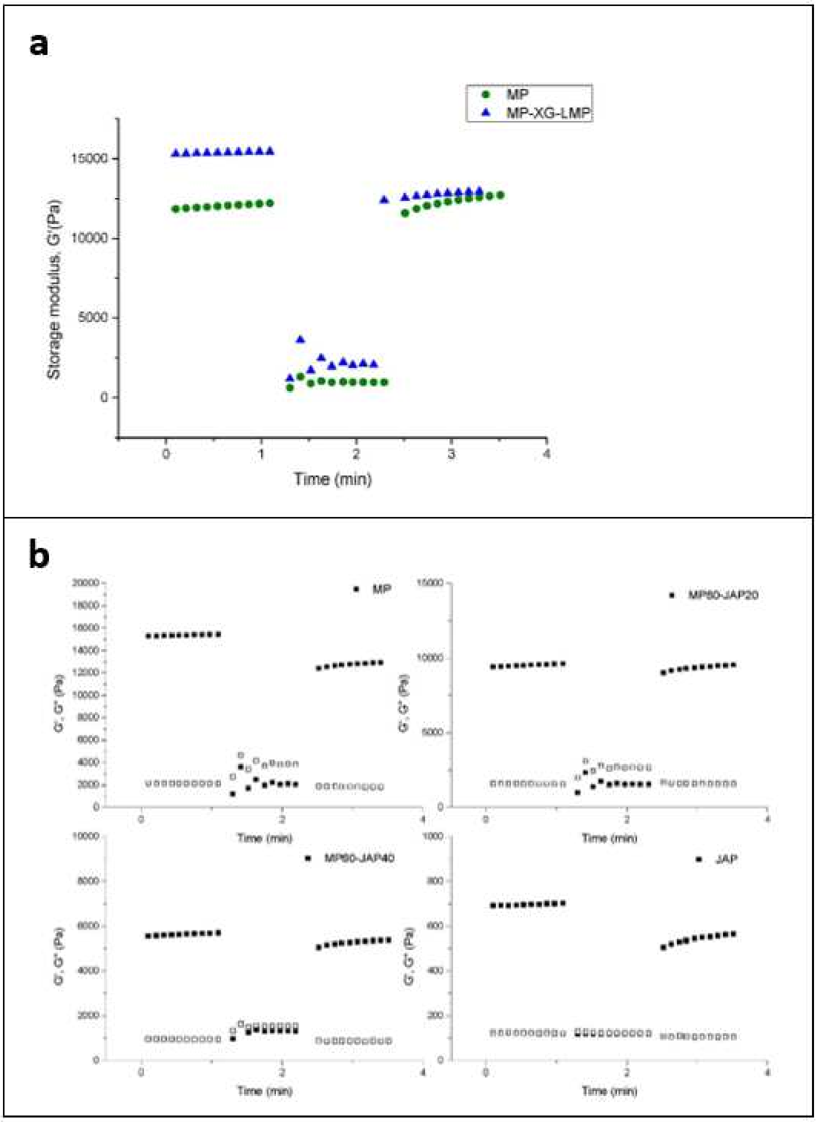

Figure 3. Three-interval time sweep test (3ITT) for extrudable pastes. The Y-axis, G' (filled symbol) and G'' (empty symbol), correspond to the storage and loss modules respectively. MP: mashed potatoes; **a:** XG: xanthan gum at 1% w/w; LMP: low methoxyl pectin at 1% w/w. **b:** JAP: Jerusalem artichoke puree; MP80-JAP20 and MP60-JAP40 represent formulations with a 20% and 40% replacement of MP by JAP.

Although all pastes were extrudable, the formulation composed exclusively of JA powder showed insufficient structural recovery to maintain the geometry of the printed parts, leading to shape collapse after deposition (**Figure 4a**). Conversely, pastes formulated with potato base and up to 40% JA replacement enabled the successful printing of stable structures, including geometries of higher complexity (**Figure 4**).

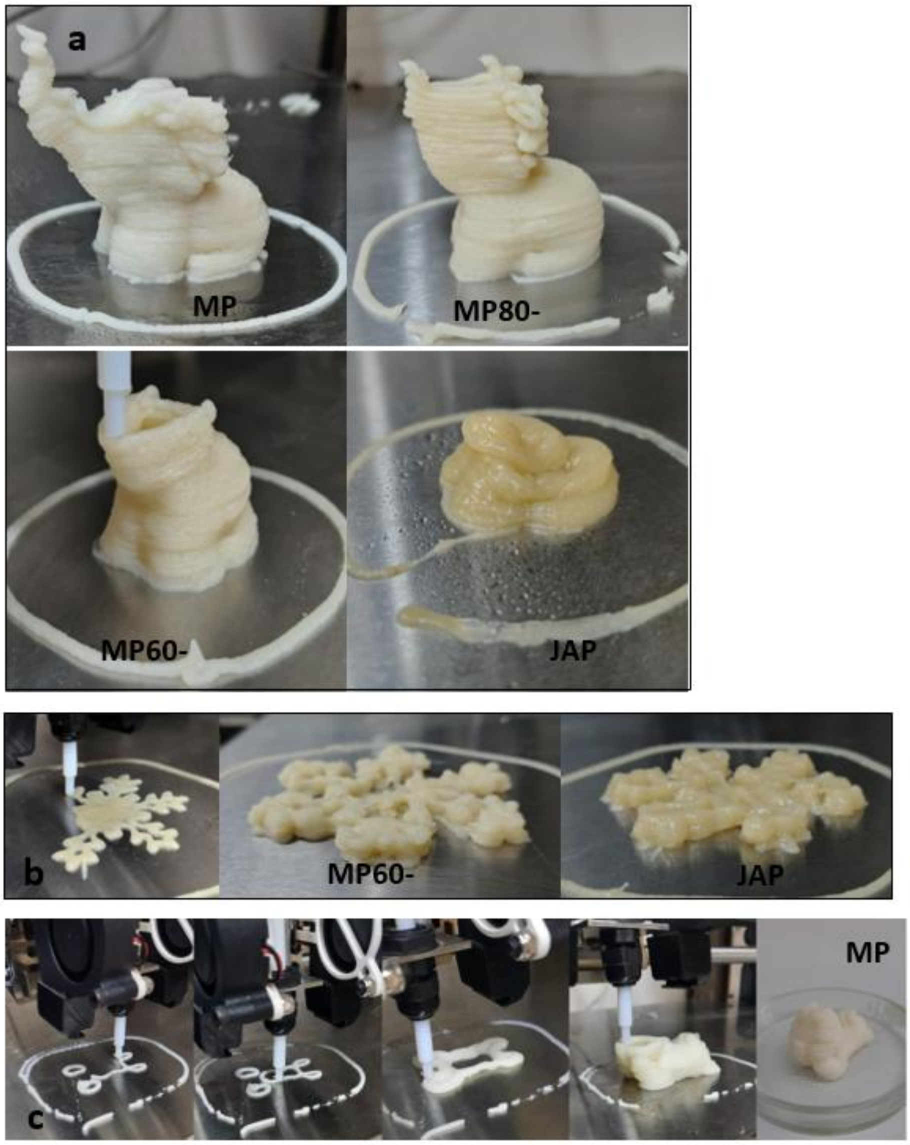

Figure 4. 3D Printing images: **a:** Illustrative images of the concept of shape fidelity. The same pattern printed with the assayed extrudable pastes with different rheological properties; **b:** Images showing the effect of the formulation of extrudable pastes on the shape fidelity of the 3D printed object with complex geometry (ice crystal). **c:** Images showing the sequence of the 3D printing process with an extrudable paste based on MP.

The combined analysis of strain sweep, frequency sweep, and three-interval thixotropy tests provides a comprehensive framework to assess printability and shape fidelity of extrudable food pastes. Alvarez-Castillo et al. (2021) developed two printability maps by correlating the rheological properties and printability of various pastes to identify the rheological characteristics required for successful printing. The first map is based on frequency sweeps, which identified that pastes with viscoelastic modules below 103 Pa or above 105 Pa would be either too weak to maintain their shape or too rigid to be correctly extruded, respectively. Based on the results obtained in the present study, the MP, MP80JAP20, and MP60JAP40 pastes exhibited adequate rheological properties for printing, whereas the JAP sample showed viscoelastic module values below the lower limit, indicating a weak paste. The second map constructed by these authors is based on flow tests, which revealed that as the shear rate increased, all printability boundaries shifted toward lower viscosity values. The flow curves obtained for the tested pastes (Figure S1) yielded values consistent with the proposed map, with the JAP formulation again being located within the printability limit regions. Evaluating the printability of different pastes through rheological results proves to be useful for making a preliminary estimation of the material application and processing.

3.4 Post-Printing Gelation and Texture Profile Analysis of Printed Products

3D-printed products are either consumed directly or subjected to post-processing which, beyond enhancing flavor, is essential for maintaining structural stability (Kadival et al 2023). Post-processing techniques are often required for 3D-printed foods to ensure both flavor development and shape retention. The effect of calcium concentration on post-printing gelation was evaluated on the MP-based formulation by means of texture profile analysis (TPA), in order to assess the development of mechanical strength and structural integrity induced by ionic crosslinking. In low-methoxyl pectin systems, Ca^{2+} ions act as junction points that promote the formation of a three-dimensional network through the well-known “egg-box” mechanism, which directly governs firmness and shape retention of the printed constructs (Coin et al., 2025).

Increasing calcium concentration from 1% to 5% (w/v) resulted in a marked increase in hardness, from 0.78 ± 0.18 N to 1.44 ± 0.44 N, indicating a progressive network reinforcement associated with a higher crosslink density. Similar results were reported by Fraeye et al. (2010).

However, further increasing $CaCl_2$ concentration to 10% (w/v) did not yield proportional gains in mechanical performance. At this level, hardness reached 1.81 ± 0.41 N, while adhesiveness showed a decrease of 0.77 ± 0.28 mJ to 0.36 ± 0.21 mJ, suggesting the development of a more brittle network likely associated with excessive ionic crosslinking and reduced chain mobility.

These results indicate the existence of an optimal calcium concentration for post-deposition gelation. From a printing perspective, moderate $CaCl_2$ levels (5% w/v) provide sufficient structural reinforcement to enhance shape fidelity of the printed constructs, whereas excessive calcium addition (10% w/v) may compromise structural resilience, increasing susceptibility to fracture or loss of integrity during handling (Capel et al., 2006). Accordingly, a $CaCl_2$ concentration of 5% (w/v) was selected for subsequent experiments as the most suitable condition to balance gel strength.

Texture profile analysis (TPA) of the printed constructs provided quantitative insight into the mechanical stability and structural integrity of the fabricated geometries. Hardness is directly associated with resistance to deformation and vertical buildability, while cohesiveness reflects the internal bonding strength between deposited layers, both of which are critical for shape fidelity in extrusion-based 3D printing (Nikolaou et al., 2025). Instrumental TPA parameters such as hardness and adhesiveness are widely used to characterize the mechanical behavior of printed food matrices and to predict their performance during handling and consumption (Pereira et al., 2021). In addition, increased firmness has been correlated with reduced dimensional deformation in printed gel systems, highlighting the role of mechanical strength in maintaining structural stability after deposition (Molina-Montero et al., 2022).

Table 2. Texture parameters obtained from the texture profile (TPA). MP: mashed potatoes; JAP: Jerusalem artichoke puree; MP80-JAP20 and MP60-JAP40 represent formulations with a 20% and 40% replacement of MP by JA powder.

Sample	Concentration of crosslinking solution	Hardness (N)	Area (mJ)	Adhesiveness (mJ)	Resilience	Cohesiveness	Elasticity
MP	5% w/v $CaCl_2$	1.41 ± 0.44^{c}	0.99 ± 0.28^{b}	0.27 ± 0.08^{c}	0.21 ± 0.03^{a}	0.69 ± 0.02^{b}	0.95 ± 0.06^{c}
MP80-JAP20		0.98 ± 0.30^{b}	0.13 ± 0.03^{a}	0.01 ± 0.01^{a}	$0.27 \pm 0.07^{a,b}$	0.61 ± 0.03^{a}	0.70 ± 0.10^{a}
MP60-JAP40		0.79 ± 0.13^{b}	0.11 ± 0.01^{a}	$0.02 \pm 0.01^{a,b}$	0.28 ± 0.05^{b}	$0.65 \pm 0.05^{a,b}$	0.83 ± 0.09^{b}
JAP		0.28 ± 0.03^{a}	0.05 ± 0.00^{a}	0.05 ± 0.02^{b}	0.32 ± 0.11^{b}	0.75 ± 0.10^{c}	1.08 ± 0.10^{d}

Note: Reported values correspond to the mean ± standard deviation

Table 2 shows the texture results obtained for the printed samples with subsequent chemical gelation. It can be observed that as the JA powder concentration increases, the network stability decreases, resulting in lower hardness. Elasticity and cohesiveness show a similar trend, being the observed values higher for JA and MP pastes than those registered for the mixtures. Adhesiveness of the samples decreases with the addition of JA. The samples with 20% and 40% JA powder showed lower adhesiveness, with the lowest percentage of JA producing the least adhesive sample, with a significant difference ($p<0.05$) (**Table 2**).

The printability assessment comprises measurements of extrudability, dimensional accuracy, and structural stability of the resulting 3D-printed constructs. (Kadival et al., 2023). Print fidelity and structural stability were evaluated by measuring the geometric parameters of the printed pieces against those of the digital print design. Based on the TPA results, it was chosen to perform the impression form reliability test with the 40% JA paste, as this paste presents a more challenging situation than single-component pastes. The results are presented in **Table 3** for a hexagonal prism design rotated along its vertical axis, demonstrating both dimensional accuracy and height retention, with deviations in radius and height below 10% (8.58 ± 0.97% and 9.27 ± 2.67%, respectively).

Table 3. Comparison between measured and the digital design geometrical parameters. Dimensions measured with digital calipers after printing with MP60JAP40 paste.

Piece	a (mm)	b (mm)	h (mm)	Top view	Front view
To print (design)	50	50	28.5	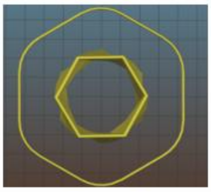	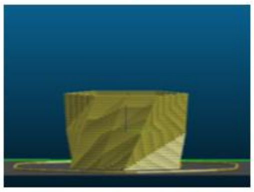
Printed	45.71±0.48	43.40±0.39	31.14±0.76	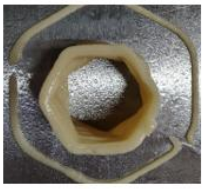	
Printed 3 hours ago	45.75±0.79	41.32±2.84	29.87±1.13		

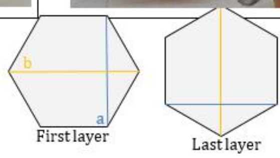

Regarding printing of complex geometries, the formulated extrudable pastes allowed for the 3D printing of complex shapes, as shown in **Figure 4**. Shape reliability was determined by the rheological characteristics of the pastes, which were not maintained in the case of pastes formulated with 100% JA powder. In pastes with up to 40% JA powder, good interlayer adhesion was observed, which conferred stability to the self-supporting parts. These observations correlate with the rheological behavior results of the pastes, particularly those from the 3TTI tests.

4. Conclusions

Extrudable pastes based on dehydrated potato flakes and Jerusalem artichoke powder were successfully formulated and their rheological behavior was systematically characterized. All formulations exhibited shear-thinning behavior with a yield stress and structural recovery after high deformation, confirming their suitability for 3D printing. The three-interval thixotropy test proved particularly effective in simulating the printing process and in assessing the ability of the pastes to rebuild their internal structure after extrusion, a key factor for shape fidelity.

Increasing JAP content led to a progressive reduction in storage and loss modules, and overall viscoelastic strength, reflecting the predominance of soluble inulin-type carbohydrates and the lower chain entanglement compared to starch-rich matrices. As a consequence, the formulation composed solely of JAP showed limited self-supporting capacity and should be therefore restricted to low-height, low-complexity geometries. In contrast, blends containing up to 40% JAP maintained adequate viscoelastic balance and recovery, enabling the printing of stable structures when combined with a xanthan gum-low-methoxyl pectin system.

Post-printing ionotropic gelation with Ca^{2+} significantly improved mechanical strength and shape retention, with the 5% $CaCl_2$ treatment providing the best balance between hardness and stability. This demonstrates the complementary roles of rheological structuring and ionic crosslinking in achieving reliable printed constructs.

From a technological standpoint, JAP represents a viable gluten-free, inulin-rich ingredient for extrusion-based additive food manufacturing. Its incorporation allows the development of printable matrices with tailored texture and enhanced functional carbohydrate content, although high structural demands still require starch-dominant networks or additional post-deposition stabilization strategies.

CRediT authorship contribution statement

DMV: Investigation; Methodology; Formal analysis; Writing - Original Draft. SZV: Conceptualization; Methodology; Validation; Supervision; Funding acquisition; Project administration; Resources; Writing - Original Draft; Writing–review and editing. MAG: Conceptualization; Investigation; Methodology; Validation; Funding acquisition; Project administration; Resources; Writing - Original Draft; Writing–review and editing. All authors discussed the results and contributed to the final manuscript. All authors read and approved the final manuscript.

Declaration of competing interest

The authors claim that they have no competing financial or personal interests that would appear to have impacted the research shown in this study.

Acknowledgments

The authors wish to thank Dr. Sebastián A. Garita and members of the FITA Group (FCAyF-UNLP) for growing and maintaining Jerusalem artichoke crops, and Dr Fernanda Hamet for the rheological measurement assistance.

Funding

This research was funded by the Agencia Nacional de Promoción Científica y Tecnológica (ANPCyT, PICT 2019-2827 IR Dr MAG and PICT 2020-1008 IR Dr SZV) and the National University of La Plata (UNLP) (Project A-375).

Data availability

The data that support the findings of this study are available from the corresponding author upon reasonable request.

References

Abu Elella, M. H., Goda, E. S., Gab-Allah, M. A., Hong, S. E., Pandit, B., Lee, S., Gamal, H., Rehman, A. U., & Yoon, K. R. (2021). Xanthan gum-derived materials for applications in environment and eco-friendly materials: A review. *Journal of Environmental Chemical Engineering*, *9*(1), 104702. https://doi.org/10.1016/j.jece.2020.104702

Afoakwah, N. A. (2022). Jerusalem artichoke (*Helianthus tuberosus*) dietary-fiber powder functionality. *Heliyon*, *8*(12). https://doi.org/10.1016/j.heliyon.2022.e12426/asset/a05e2ac8-d079-4b5b-ae1e-5983908e5348/main.assets/gr5.jpg

Álvarez-Castillo, E., Oliveira, S., Bengoechea, C., Sousa, I., Raymundo, A., & Guerrero, A. (2021). A rheological approach to 3D printing of plasma protein based doughs. *Journal of Food Engineering*, 288, 110255. https://doi.org/10.1016/j.jfoodeng.2020.110255

Bohórquez Montoya, C. J. (2018). *Impacto de las propiedades viscoelásticas y estructurales en la impresión 3D de hidrocoloides de almidón-mango y almidón-arabinoxilanos*. https://hdl.handle.net/1992/44280

Cai, L., Feng, L., Nie, M., Li, D., Zheng, T., & Zhang, M. (2023). Effect of different hydrocolloids on the rheological, microstructural, and 3D printing characteristics of purple sweet potato puree. *Food and Bioprocess Technology,* 16, 2622–2634. https://doi.org/10.1007/s11947-023-03085-2

Capel, F., Nicolai, T., Durand, D., Boulenguer, P., & Langendorff, V. (2006). Calcium and acid induced gelation of (amidated) low methoxyl pectin. *Food Hydrocolloids*, *20*(6), 901–907. https://doi.org/10.1016/j.foodhyd.2005.09.004

Coin, F., Larrañaga, A., & Cerveny, S. (2025). Structural characterization of low methoxyl pectin-based adsorbents: the role of water on pectin structure. *Carbohydrate Polymer Technologies and Applications*, *11*, 100885. https://doi.org/10.1016/j.carpta.2025.100885

Cui, Y., Li, C., Guo, Y., Liu, X., Zhu, F., Liu, Z., Liu, X., & Yang, F. (2022). Rheological & 3D printing properties of potato starch composite gels. *Journal of Food Engineering*, *313*, 110756. https://doi.org/10.1016/j.jfoodeng.2021.110756

del-Mazo-Barbara, L., & Ginebra, M. P. (2021). Rheological characterisation of ceramic inks for 3D direct ink writing: A review. *Journal of the European Ceramic Society*, *41*(16), 18–33. https://doi.org/10.1016/j.jeurceramsoc.2021.08.031

Di Rienzo, J., Casanoves, F., Balzarini, M., Gonzalez, L., Tablada, M., & Robledo, C. (2011). InfoStat versión 2011. *Grupo InfoStat, FCA, Universidad Nacional de Córdoba, Argentina.*

Fraeye, I., Colle, I., Vandevenne, E., Duvetter, T., Van Buggenhout, S., Moldenaers, P., Van Loey, A., & Hendrickx, M. (2010). Influence of pectin structure on texture of pectin–calcium gels. *Innovative Food Science & Emerging Technologies*, *11*(2), 401–409. https://doi.org/10.1016/j.ifset.2009.08.015

Hakim, L., Deshmukh, R. K., Lee, Y. S., & Gaikwad, K. K. (2024). Edible ink for food printing and packaging applications: a review. *Sustainable Food Technology*, *2*(4), 876–892. https://doi.org/10.1039/d4fb00036f

Hu, H., Guo, J., Huang, Z., Huang, Q., & Lu, X. (2023). Effect of different hydrocolloids on the physicochemical, printing, and digestion properties of 3D printed purple sweet potato. *Food Hydrocolloids*, *144*, 109058. https://doi.org/10.1016/j.foodhyd.2023.109058

Jeon, E. Y., Kim, Y., Yun, H. J., Kim, B. K., & Choi, Y. S. (2024). 3D Printing of Materials and Printing Parameters with Animal Resources: A Review. *Food Science of Animal Resources*, *44*(2), 225. https://doi.org/10.5851/kosfa.2023.e73

Juszczak, L., Witczak, T., Ziobro, R., Korus, J., Cieślik, E., & Witczak, M. (2012). Effect of inulin on rheological and thermal properties of gluten-free dough. *Carbohydrate Polymers*, *90*(1), 353–360. https://doi.org/10.1016/j.carbpol.2012.04.071

Kavidal, A., Kour, M., Meena, D., & Mitra, J. (2023). Extrusion-nased 3D food printing: printability assessment and improvement techniques. *Food and Bioprocess Technology,* 16, 987–1008. https://doi.org/10.1007/s11947-022-02931-z

Karimi, R., Azizi, M. H., Ghasemlou, M., & Vaziri, M. (2015). Application of inulin in cheese as prebiotic, fat replacer and texturizer: A review. In *Carbohydrate Polymers* (Vol. 119, pp. 85–100). Elsevier Ltd. https://doi.org/10.1016/j.carbpol.2014.11.029

Kaur, N., & Gupta, A. K. (2002). Applications of inulin and oligofructose in health and nutrition. *Journal of Biosciences*, *27*(7), 703–714. https://doi.org/10.1007/bf02708379

Letras, P., Oliveira, S., Varela, J., Nunes, M. C., & Raymundo, A. (2022). 3D printed gluten-free cereal snack with incorporation of Spirulina (*Arthrospira platensis*) and/or Chlorella vulgaris. *Algal Research*, *68*. https://doi.org/10.1016/j.algal.2022.102863

Liu, Z., Bhandari, B., Prakash, S., & Zhang, M. (2018). Creation of internal structure of mashed potato construct by 3D printing and its textural properties. *Food Research International*, *111*, 534–543. https://doi.org/10.1016/j.foodres.2018.05.075

Liu, Z., Zhang, M., Bhandari, B., & Wang, Y. (2017). 3D printing: Printing precision and application in food sector. *Trends in Food Science & Technology*, *69*, 83–94. https://doi.org/10.1016/j.tifs.2017.08.018

Liu, Z., Zhang, M., Bhandari, B., & Yang, C. (2018). Impact of rheological properties of mashed potatoes on 3D printing. *Journal of Food Engineering*, *220*, 76–82. https://doi.org/10.1016/j.jfoodeng.2017.04.017

Megusar, P., Stopar, D., Poklar Ulrih, N., Dogsa, I., & Prislan, I. (2022). Thermal and Rheological Properties of Gluten-Free, Starch-Based Model Systems Modified by Hydrocolloids. *Polymers*, *14*(16). https://doi.org/10.3390/polym14163242

Mezger, T. (2020). *The rheology handbook: for users of rotational and oscillatory rheometers* (5th ed.).

Molina-Montero, C., Matas, A., Igual, M., Martínez-Monzó, J., & García-Segovia, P. (2022). *3D Food Printing: Effect of Apricot Pulp Concentration on Texture Analysis Profile and Image Analysis in a Gel Cylinder*. 72. https://doi.org/10.3390/foods2022-12950

Nikolaou, E. N., Apostolidis, E., Nikolidaki, E. K., Karvela, E. D., Stergiou, A., Kourtis, T., & Karathanos, V. T. (2025). The Development and Optimization of Extrusion-Based 3D Food Printing Inks Using Composite Starch Gels Enriched with Various Proteins and Hydrocolloids. *Gels 2025, Vol. 11, 11*(8). https://doi.org/10.3390/gels11080574

Paseephol, T., Small, D. M., & Sherkat, F. (2008). Rheology and texture of set yogurt as affected by inulin addition. *Journal of Texture Studies*, *39*(6), 617–634. https://doi.org/10.1111/j.1745-4603.2008.00161.x

Pereira, T., Barroso, S., & Gil, M. M. (2021). Food texture design by 3d printing: A review. In *Foods* (Vol. 10, Number 2). MDPI AG. https://doi.org/10.3390/foods10020320

Prithviraj, V., Díaz, L. P., Lemus-Mondaca, R., Ullah, A., & Roopesh, M. S. (2025). Emerging advancements in 3D food printing. *Frontiers in Food Science and Technology*, *5*, 1607449. https://doi.org/10.3389/frfst.2025.1607449

Qin, Z., Yang, Y., Zhang, Z., Li, F., Hou, Z., Li, Z., Shi, J., & Shen, T. (2025). A Critical Review: Gel-Based Edible Inks for 3D Food Printing: Materials, Rheology–Geometry Mapping, and Control. *Gels 2025, Vol. 11, 11*(10). https://doi.org/10.3390/gels11100780

Rubel, I. A., Iraporda, C., Novosad, R., Cabrera, F. A., Genovese, D. B., & Manrique, G. D. (2018). Inulin rich carbohydrates extraction from Jerusalem artichoke (*Helianthus tuberosus* L.) tubers and application of different drying methods. *Food Research International*, *103*, 226–233. https://doi.org/10.1016/j.foodres.2017.10.041

Shariati, M. A., Khan, M. U., Hleba, L., Souza, C. K. de, Tokhtarov, Z., Terentev, S., Konovalov, S., Arduvanova, F., Batishcheva, N., Shigapov, I., Ekaterina, S., & Kantimerova, M. (2021). Topinambur (the *Jerusalem artichoke*): nutritional value and its application in food products: an updated treatise. *Journal of Microbiology, Biotechnology and Food Sciences*, *10*(6), e4737–e4737. https://doi.org/10.15414/jmbfs.4737

Sun, J., Zhou, W., Huang, D., Fuh, J. Y. H., & Hong, G. S. (2015). An Overview of 3D Printing Technologies for Food Fabrication. *Food and Bioprocess Technology 2015 8:8*, *8*(8), 1605–1615. https://doi.org/10.1007/s11947-015-1528-6

Uribe-Wandurraga, Z. N., Igual, M., Reino-Moyón, J., García-Segovia, P., & Martínez-Monzó, J. (2021). Effect of Microalgae (*Arthrospira platensis* and *Chlorella vulgaris*) Addition on 3D Printed Cookies. *Food Biophysics*, *16*(1), 27–39. https://doi.org/10.1007/S11483-020-09642

Vega, D. M., Versino, F., Dini, C., Viña, S. Z., & García, M. A. (2024). Gluten-free baked products formulated with Jerusalem artichoke (*Helianthus tuberosus*) flour. *International Journal of Gastronomy and Food Science*, *36*, 100946. https://doi.org/10.1016/J.IJGFS.2024.100946

Whitcomb, P. J., & Macosko, C. W. (1978). Rheology of Xanthan Gum. *Journal of Rheology*, *22*(5), 493–505. https://doi.org/10.1122/1.549485

Witczak, T., Witczak, M., & Ziobro, R. (2014). Effect of inulin and pectin on rheological and thermal properties of potato starch paste and gel. *Journal of Food Engineering*, *124*, 72–79. https://doi.org/10.1016/j.jfoodeng.2013.10.005

Zhu, W., Iskandar, M. M., Baeghbali, V., & Kubow, S. (2023). Three-Dimensional Printing of Foods: A Critical Review of the Present State in Healthcare Applications, and Potential Risks and Benefits. *Foods 2023, Vol. 12, Page 3287*, *12*(17), 3287. https://doi.org/10.3390/foods12173287

Supplementary Files

This is a list of supplementary files associated with this preprint. Click to download.

- GraphicalabstractVegaetal2026PNG.png